Failure-mode Metrology using Projected Target Videogrammetry

By
[1]John A. Greenwood, [2]Christine Darve, [1]Robert Bernstein, [3]Edgar Black and [4]Donna Kubik
[1] Fermi National Accelerator Laboratory, Batavia, IL, USA
[2] Northwestern University, Evanston, IL
[3] Illinois Institute of Technology, Chicago, IL
[4] Northern Illinois University, DeKalb, IL

Abstract:

Future particle accelerators are being researched today. One such machine is the Muon Collider under study at Fermi National Accelerator Laboratory and in several other national and international High-Energy Physics laboratories. A central component of the Muon Collider is the Liquid Hydrogen (LH_2) Absorber, used to cool the muon beam. The LH_2 Absorber is a cylindrical container filled with liquid hydrogen through which the muon beam will be transmitted in order to depose its transverse energy. The LH_2 Absorber end caps, or windows, are specially designed aluminum spherical domes of tapered thickness. It is designed to contain the pressurized LH_2 and, at the same time, permit the passage of the muon beam with a minimum resistance or energy loss. A finite element analysis (FEA), modeling the behavior of the window design, was used to validate the results of this analysis. A window with 0.13 mm at the minimum thickness was machined and tested by pressurizing it with water up to rupture. Results of the test were compared with the FEA predictions, thereby creating an accurate model for the future design of various sizes of Absorber windows. Anticipating the need to accurately measure the characteristics of a production series of windows, without the use of strain gages or other means in direct contact with the surface, a digital photogrammetry process was incorporated to measure the displacement of the Absorber window while under pressurization. The displacement measurements, as determined by photogrammetry, were correlated with the FEA and strain gauge measurements, are used to validate the Absorber window design. This paper discusses the metrology of surface behavior during destructive testing of the LH_2 Absorber Window using projected target digital photogrammetry.

1 BACKGROUND

One of the next steps toward the understanding of the high-energy physics theories is the use of high luminosity muon beams [1-2]. The proposal of the muon collider experiment is developed from this aspiration**.** Later, these developments will lead to its use as a component for a neutrino factory muon storage ring.

- What is a Muon and where do Muons come from? Like the electron, the muon belongs to the family of the leptons. The muon mass is equal to $1.86 \cdot 10^{-34}$ kg. It has a mass ~210 times heavier than the electron, hence it possesses a larger energy. Being more energetic makes it a good candidate for searching for fundamental particles. Muons are produced by a proton interacting with a target containing liquid (with a high atomic number, Z), which produces a pion+ and pion- couple that, subsequently, decay into muon+, muon-. Muons decay into neutrino and electron.

- What is a Muon Collider? The muon collider is composed of a proton source, a target, lithium absorber, a Linac (Linear Accelerator made up of RF cavities, solenoids and LH_2 absorbers) and a storing ring with collider. The muon beam is created by a proton source being accelerated through a Linac; it releases its energy by ionization cooling along the cooling channel in the LH_2 absorbers. The collider is a region of the machine where the actual collisions of the muons and their antimatter partners take place, and where the products of the collisions are detected. The purpose behind colliding muons is linked to the search of the Higgs Boson. The second purpose of the Muon Collider is to provide muon storage in order to direct the neutrino issued from the muon decay, toward various worldwide detectors in the process of understanding the neutrino oscillations.

- What do you get when you collide muons? Different kinds of elementary particles (quarks, fermions, bosons.) will be issued from the collisions, dependent upon the energy at the center of mass of the two-muon beams.

- Why do you cool Muons and, maybe more importantly, how do you cool them? In order to operate the muon beam in proper conditions, the phase-space volume occupied by the initial beam needs to be reduced. The proposed technique of ionization cooling expects to reduce it by a factor 10^5- 10^6. For this purpose, liquid hydrogen (LH_2)

absorbers are chosen and inserted in the Muon Collider's cooling channel. The beam needs to depose its transverse energy (dE/dx) in the LH_2 absorber. The muons traverse the hydrogen volume in which they lose both longitudinal and transverse momentum due to ionization losses. The longitudinal momentum is replaced by using the RF accelerating cavities and solenoid magnets. Figure 1 shows two of the 43 modules of the cooling channel, composing a portion of the 218-m subsystem.

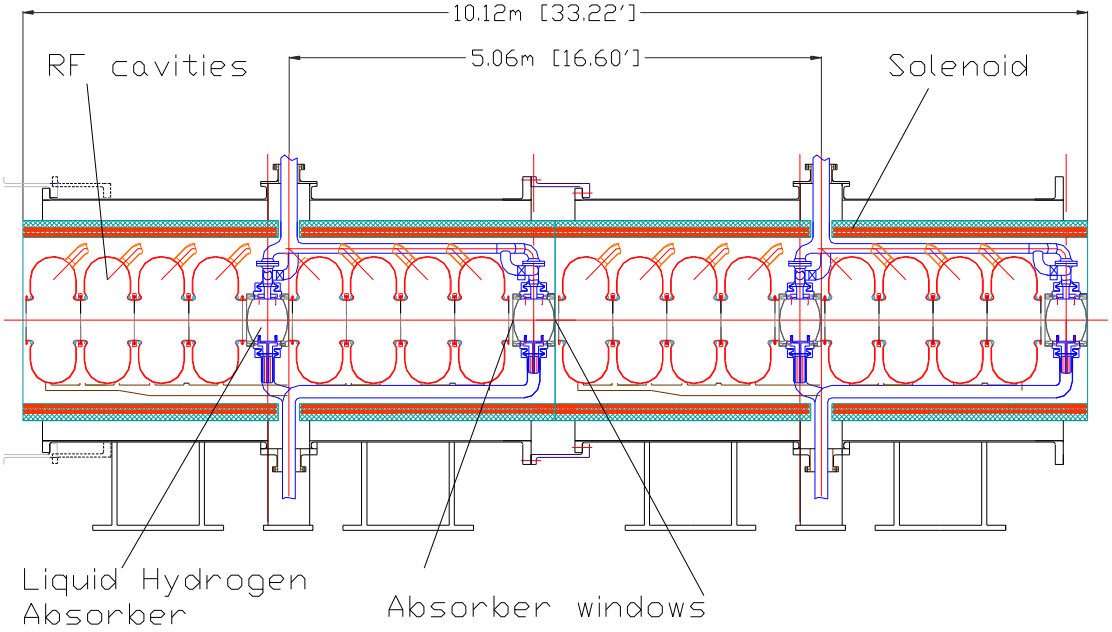

Figure 1: Two modules of the double field flip cooling channel

- Why use liquid hydrogen? Because Hydrogen has a very low atomic number and the usefulness of the medium diminishes as the square of the atomic number. Helium, for example, has an atomic number of 2, while Hydrogen's atomic number is 1, which makes Hydrogen four times more effective than Helium.

- How is the Absorber window fabricated and why so thin? Turning aluminum stock on a lathe makes the Absorber Window. The 20-mm diameter circle at the center of the dome is thinner than the edges. It is thin in order to minimize losses when the beam passes through the aluminum. One might ask why not use Beryllium, which has some better material properties? Beryllium, which has some better material properties, was rejected because it is very hazardous; if the LH_2 should explode, the Beryllium particles would create a very severe situation. For more information, see the appendix.

- Why the test needs to be destructive? The FNAL safety review panel requires a test up to the rupture point for at least one prototype in order validate the design of the Absorber window. The test can be at room temperature considering that properties of materials increase in strength at cryogenic temperatures. The design will be validated if the predictions of the Finite Element Analysis (FEA) model agree with the test results. The calculation and destruction of the window will validate the process of manufacturing the windows in production.

2 DESIGN OF THE ABSORBER WINDOW

The LH_2 absorber window design developed by Edgar Black, IIT project managing engineer, is based on the ASME and the FNAL safety recommended requirements. It can be described as a pair of nearly osculating spheres of slightly different curvature radius [3]. Several Absorbers, with similar windows of various diameters, will equip the Muon Collider cooling channel. In this study, we focus on the LH_2 Absorber design with 15-cm radius windows. The proposed design specifies a maximum allowable working pressure of 1.2 atmospheres. The FEA results predict that a 0.29-mm thick

window for this requirement. Similar calculations were performed for other different window dimensions. A 0.13-mm thick window was fabricated first in order to verify the manufacturing feasibility of such thin aluminum parts. In the subject 0.13-mm thick window, the concave surface has a curvature radius of 30 cm, while the convex surface has a curvature radius of 30.844 cm (see figure 2). The center points of the two spheres are offset by 0.832 cm along the principal axis of the window (the muon beam direction). This means that the thickness of the window varies from 0.94 mm just inside the fillet at the interior base of the mounting flange, down to 0.13 mm at the center – approximately the width of two human hairs placed side-by-side.

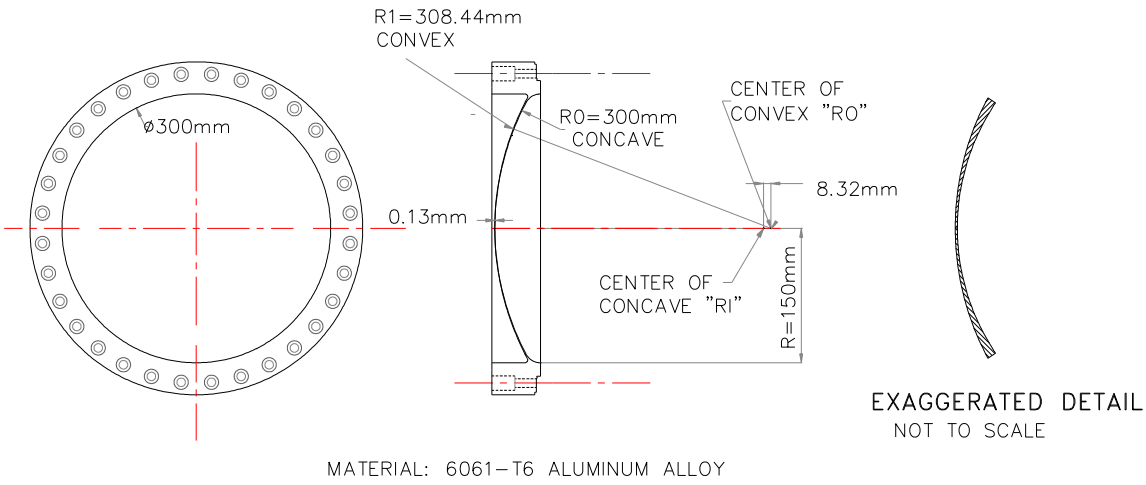

Figure 2: Design of the LH_2 absorber window

3 PURPOSE OF THE PRESSURE TEST

The pressure test permits the investigation of the behavior of the LH_2 Absorber window, while applying water pressure to the window's concave side. This preliminary test is performed at room temperature. Later, liquid nitrogen temperature tests are foreseen. The pressure simulates the Muon Collider operating conditions. The mechanical behavior of the aluminum window in its elastic mode is determined by means of strains and displacements directly measured on the convex side of the window. These measurements are correlated to the FEA results. The LH_2 Absorber window is modeled using FEA, which predicts the stress, the strain and the displacement of the LH_2 Absorber window while pressurized. The validation of the calculations is part of the process of acceptance for the manufacturing of the series of windows.

The purpose of the test is to measure and analyze the strains and the displacements of the window surface as it reacts to successively greater pressure, applied in discrete steps to the window's concave side until rupture. The measurement of the displacement by the digital photogrammetry is complementary to the strain measurement. Both measurements are used in parallel. The photogrammetric process measures displacements in a range of pressure larger than can be reliably measured with strain gages.

This test also permits us to evaluate the future procedure of production inspection. The important qualities of the test are: non-contact, reliable, and relatively straightforward measurements. It allows us to foresee the inspection of a production series of windows without the use of strain gages, which are always complicated when install on such fragile surfaces. After the validation of the window design, the production windows will need to be pressurized up to the maximum allowable working pressure before being implemented in the cooling channel. This test allows us to learn and develop an optimal procedure for the rapid inspection of a large series of windows.

4 DESCRIPTION OF THE TEST SETUP

The 0.13-mm thick window is assembled to a back plane. Eight liters of water is used to fill the volume between the back plane and the concave side of the window. The water circuit permits us to pressurize the concave side of the window. Twenty-two strain gages are bonded on the convex side of the window. Figures 3 and 4 show the installation of the strain gages on the LH_2 Absorber window. The DAQ system permits us to record the strain and the pressure signals at 1 ms time interval. The DAQ system made direct resistive measurements (Keithley 2700 DVM) of the strain gages as well as half-bridge voltage measurements (National Instruments 5B38 modules through both the DVM and National Instruments PCI-MIO-16E ADC modules at 10 Hz and 1kHz respectively). The LH_2 Absorber window, with its instrumentation and pressurization circuit, is installed on an optical bench. The schematic of the setup of the absorber window pressure test is shown in figure 5.

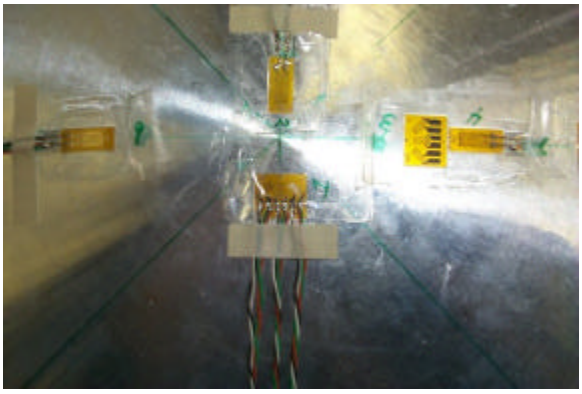

Figure 3: Installation of the strain gages

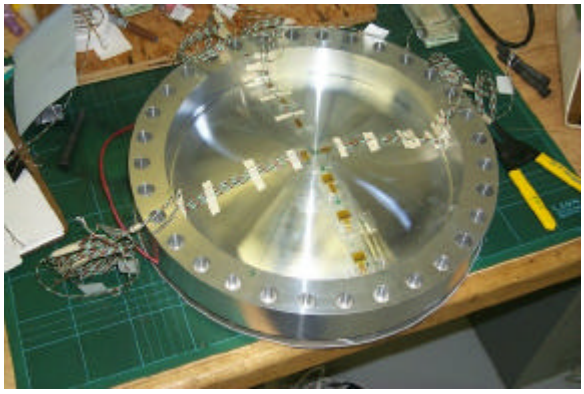

Figure 4: Preparation of the window

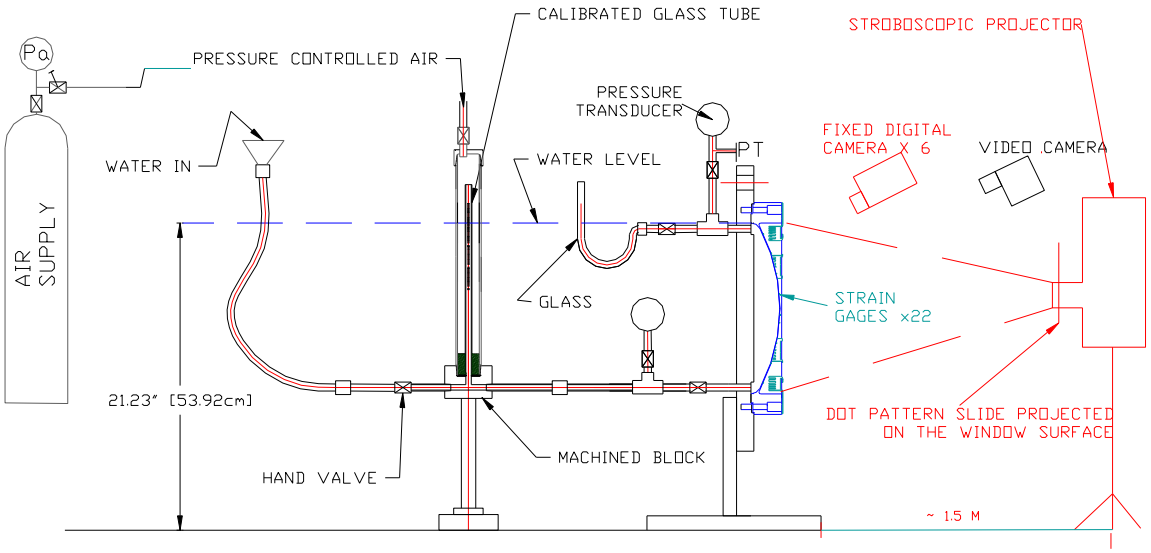

Figure 5: Setup of the absorber window pressure test

The measurement of the displacement must be accurate, without use of any device that makes contact with the window**,** with fast acquisition of a large number of discrete points on the LH_2 Absorber window surface. One of the main arguments for the choice of photogrammetry is the non-contact measurement capability and the large surface coverage. Several alternative measurement strategies were discussed – high speed cameras, laser interferometer, laser scanning – but each was discounted for various reasons e.g. the high speed cameras offer little or no measuring capability, the laser

interferometer, while measuring quite accurately, doesn't give much coverage, and the laser scanner doesn't produce the resolution required. Since the aluminum window is in some places as thin as 0.13 mm, the use of reflective stickers needed for the traditional photogrammetry measurements would disturb the measurement itself. In addition, the window's surface finish is not compatible with the direct laser measurement. While, ultimately, single camera digital videogrammetry was selected, we reviewed the suitability of the multi-camera videogrammetry approach, as well. We rejected the latter as having fundamentally less accuracy and the budgetary burden associated with having a sufficient number of cameras to afford optimal coverage.
For the purpose of the photogrammetry test, the window's convex side has been coated with a non-destructive testing developer and a pattern of dots was projected on the surface with a stroboscopic projector located 1.5 m away from the window assembly.

5 THE PHOTOGRAMMETRY TECHNIQUE

The material used for the photogrammetry test [4] is a stroboscopic projector and a metric digital camera, plus all the associated targeting devices. Figure 6 shows the stroboscopic projector. Figure 7 shows the digital camera. Figure 8 shows the setup for the photogrammetric measurements with the stroboscopic projector, the digital camera, and the window setup. In any photogrammetric mission, targeting and camera locations are the primary issues, followed closely by the required number of exposures. The first strategy was to place a series of adhesive strip targets along several radial lines on the convex surface. This was rejected for four reasons: 1) the window surface is so delicate that any unnecessary handling must be eliminated, 2) a number of strain gages would be occupying part of the surface real estate (see Figure 4), 3) the adhesive strips would actually act as support for the surface, and 4) the strips, being a planar element, would cusp on a spherical surface, thereby causing irregular reflections from the targets on the strips.

As luck would have it, a new accessory for videogrammetry has become available in the past year. This is a target projector that is strobed in synchronization with the camera. A slide with the appropriate target pattern and density is used, which can range from 650 to 5600 dots. The projected dots are a direct, non-contacting substitute for the strip targets. The diameter of the slide is 85 mm and the dot diameter on the slide is 0.20 mm. The projected dot diameter and coverage is a function of the distance from the part to the projector. Since our plan called for 3 mm coded targets, we selected a projected dot size of 3 mm, as well. Figure 9 shows the window and the projected dots on the convex side.

The method of simulating liquid hydrogen pressurization of the Absorber window is to seal the concave sides with a flat plate, fill the space with water, and then increase the pressure on the water in steps. A base measurement is made with no pressure applied, then, successively increasing the pressure in steps of one-tenth of the range to a point slightly above the predicted failure point. At each step, the Absorber Window is allowed to stabilize, and then a sequence of exposures is taken, along with the strain gage readings.

Figure 6: Stroboscopic projector

Figure 7: Digital camera

Figure 8: Setup of the photogrammetry test

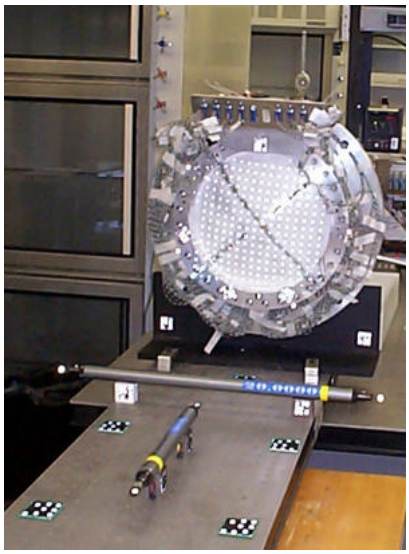

Figure 9: Scale bars and dot pattern

An important consideration presents itself at this point. Since the plan is to measure at least eleven correlated epochs, (the base measurements plus ten, or more, steps in pressure) our interest is in the change in surface position of each of the projected targets, we want the X and Z location of the dots (with Y being the principal axis (beam axis) of the Absorber window) to remain fixed with respect to the reference frame (not only during each single epoch, but also during the duration of all eleven epochs). Forcing this requirement allows the determination of the displacement of the surface to be made in a single axis, while the X and Z values, which should remain stationary, provide a check on the overall stability of the setup. To accomplish this objective, one large optical bench was installed in the work area, with the LH_2 Absorber window, the stroboscopic projector and the controls for pressurizing the window mounted on.

A further condition when using the projector reared its ugly head: that of needing to work with the camera on a tripod. Those not familiar with modern videogrammetry immediately assume that a tripod is a required accessory. This is generally not the case because the flash is strobed for such a short period of time that image motion is not an issue. However, with the projector, the flash used to illuminate the reference targets precedes the projector flash by about ten milliseconds. With a 24 ms overall exposure time, this is sufficient time for apparent motion to occur for the projected targets relative to the reference targets when taking hand-held exposures.

In the end, it became clear that many more than the originally planned eleven epochs would be taken and the time to acquire the images would need to be as short as possible. A total of thirty-five steps in pressure were measured over a period of two and one-half hours. Each epoch was to be measured in approximately one minute; with the remainder of the time being spent increasing the pressure, making pressure measurements, and allowing the system to stabilize. The use of a tripod to support the digital camera, while having the potential of increasing the time to acquire the exposures, permits us to reduce the number of exposures necessary to produce accurate results.

A base set of 50 exposures was made of all the control targeting, scale bars, and coded targets, but without using the projector. The photogrammetric measurement at each pressure epoch consisted of six tripod-based exposure stations with dots being strobed onto the window surface. Because this is a differential measurement, a reasonable attempt was made for these six exposure stations to be in the same location for each epoch.

The initial fifty exposures were processed as a unit to establish a measure of the stability of the test apparatus. At the conclusion of the test, an equivalent set of exposures was taken and compared with the base set to determine if any corrections should be applied as a function of time. This comparison, constrained only by the length of the scale bars and the reference frame orientation, produced RMS accuracy estimates of 0.003 in X, Y, and Z (mm), with maximums of 0.007, 0.004, and 0.005 (mm), respectively; certainly low enough to avoid any futzing with the data for temporal causes. The Plan Quality Factor was 1.11. (The Plan Quality Factor is a global measure of how good the network was. Typically,

the Plan Quality Factor should be between 1-2. Values exceeding 2 indicate less than ideal geometry or overlap, or a poor calibration.) A template project was made from the base set exposures, plus the names and nominal coordinates of the projected targets. As part of the template project preparations, all spurious scans were removed from the base set exposures in order to minimize unwanted target solutions (those that were neither control points nor projected targets of interest). Processing of the photogrammetric data for each epoch was done by combining the fifty exposures from the base set with those exposures from each epoch. The software's Auto Measure feature allows processing only new exposures when it is restarted with the Continue function. As a result, almost no cleanup was required, and that was limited to just six exposures. Once the template project was built, processing of each epoch rarely required as long as ten minutes, which included file manipulation, exposure cleanup, bundle processing, and inspection of the of the bundle results. After eliminating unsuitable targets (more on this below), RMS accuracy estimates were in the range of 0.005, 0.007, and 0.004, with maximums generally below 0.010 mm (a rare 0.012 would slipped in twice, plus one of 0.009). The Plan Quality Factor hovered around 1.08, while the RMS of measurements was generally around 0.17 μm, and always below 0.20 μm.

Any time photogrammetric measurements are made where other instrumentation is being used, a clash of purposes ensues. In this case, strain gages and their associated wiring were the culprits. The expressed wish of the experimenters were to have the dots projected as close the strain gages as possible so that correlating the data would be simplified. The problem was that as the window expanded, the strain gages and wires moved laterally while the projected targets stayed stationary (in X-Z). Ultimately, several projected targets needed to be eliminated because the centroid of the reflection was being biased or obscured by these objects. This occurred on less than 5% of the nearly 200 useable surface targets.

6 RESULTS

6.1 Finite element analysis (FEA)

The FEA approach permits us to simulate the displacements, strain and stress on the LH_2 Absorber window surface for various pressures applied to its concave side. Preliminary to this pressure test, a tension test was performed on aluminum 6061 T6 specimen in order to measure the properties of the aluminum window. The FEA calculations make use of the Al 6061 T6 properties and simulate only the LH_2 Absorber window's behavior in the elastic mode. Figure 10 shows the axi-symmetric representation of the model. The boundary conditions consist of suppressing the degree of freedom of the flange bottom plane. The pressure is applied to the concave side of the window (see the red arrows on Figure 10). The reference system and the meshing of the LH_2 Absorber window are also illustrated.

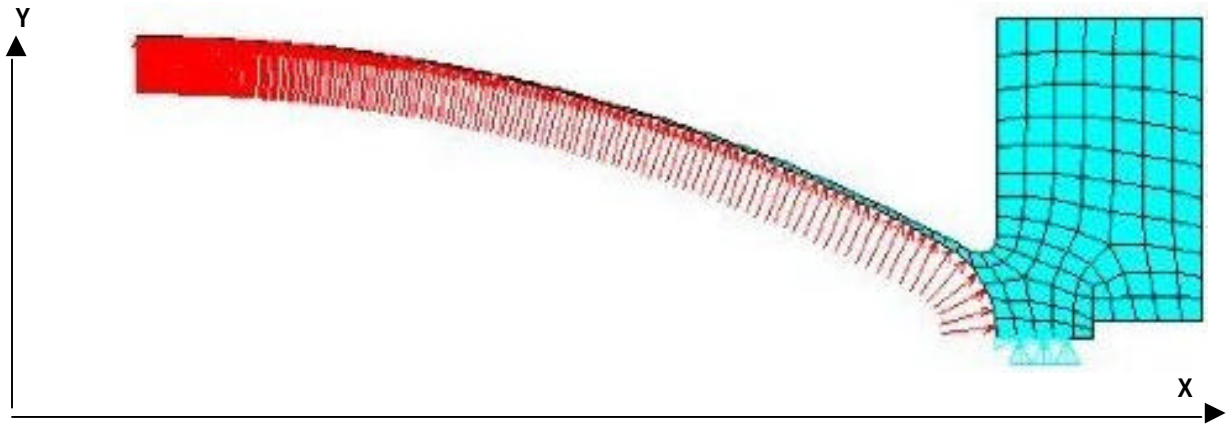

Figure 10: Axi-symmetric model of the window for the Finite Element Analyses

Figure 11 shows the distribution of the displacements along the X-axis (radial-smaller) and Y-axis (larger) for an applied pressure of 0.12 MPa. The displacements are plotted vs. the radius length of the 150-mm LH_2 absorber window. The center of the window exhibits the larger displacements along Y-axis, while the displacements along X-axis are larger in the 90-mm wide "doughnut-shaped" region, which has an inner diameter of 22 mm. The displacements in the center of the window along the X-axis are one order of magnitude smaller than the displacements along the Y-axis.

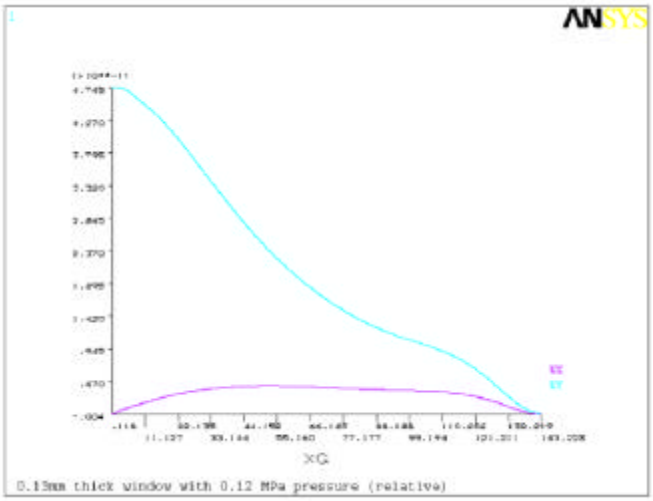

Figure 11: Distribution of the displacements along the150-mm LH_2 absorber window's radius

Figure 12 shows an axi-symmetrical view of the exaggerated deflection of the LH_2 absorber window along the Y-direction, when a 0.12MPa relative pressure is applied. The color gradient illustrates that the thick flange doesn't deflect with the pressure, whereas the center of the window witnesses a greater displacement along the Y-axis. Since we can calculate the displacement at the pressure relative to the yield of the material, we can predict the volume of water, which is used to pressurize the window from 0 PSIg to 29 PSIg. 25 ml of water was estimated and 23.8 ml was measured for a pressure of 29 PSIg.

The larger displacement is along the Y-axis: UY=448 μm for a 0.12 MPa pressure applied on the concave side of the LH_2 Absorber window

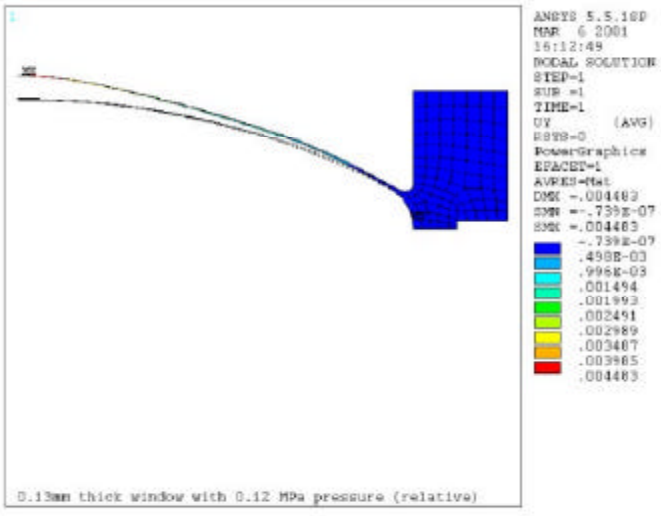

Figure 12 shows an exaggerated view of the window's nodes displacement compared to its initial position.

6.2 Photogrammetry measurements

The measurement of the strain and the displacement were carried on, up to the rupture of the window. The displacements were measured for each pressure step using photogrammetry. Figure 13, 14, 15 and 16 show the displacement along the Y-axis for the pressure of 7, 17, 31 and 36 PSIg, respectively. The sphere illustrates the convex surface of the window and permits us to build the supports for the displacement vectors. The measurements of the window with no pressure applied represent the initial measurements. The vectors shown on the following figures are determined by using the coordinate of the absolute position of each of the dots at the initial epoch and the coordinates of each point at successive steps of pressure applied to the LH_2 absorber window. The vector's color scale illustrates displacement values from 0 μm (blue) to 800 μm (red). A scale factor of 250 has been applied to the displacement values in order to make it visible. Figure 13 shows that the displacements along the Y-axis are already perceptible for a small pressure equal to 7 PSIg. The larger displacements are located in the center of the window. The pressure is homogeneously distributed on the window. Therefore, it infers larger forces on the thinner parts of the window, which is the center. The largest displacement expressed in Figure 16 is 806 μm and is located in the center of the window.

Figure 17 shows a 3-D view of the displacements along the Y direction. The symmetry of the displacement is illustrated.

As stated above, the worst RMS of the measurement is 12 μm, measured along the Y-axis. For the set of displacements measured with 36 PSIg, the RMS was 11 μm. The values that are cited in Section 5 demonstrate the fundamental reliability of projected target photogrammetry.

Views of the displacement along Y-axis with the photogrammetry technique.

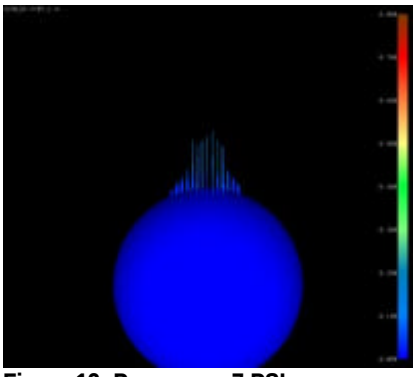

Figure 13: Pressure = 7 PSIg

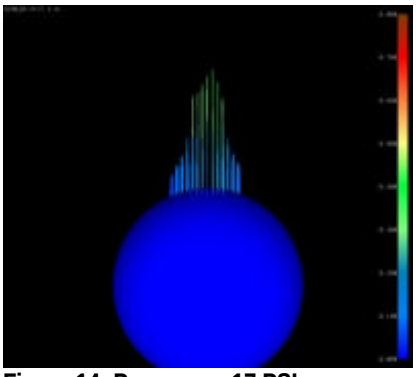

Figure 14: Pressure = 17 PSIg

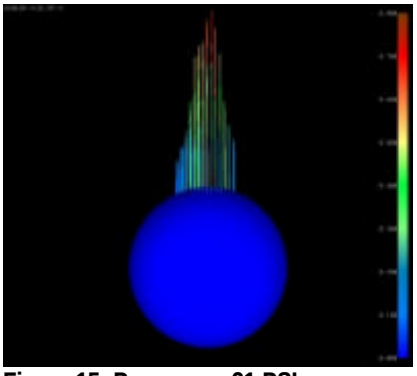

Figure 15: Pressure = 31 PSIg

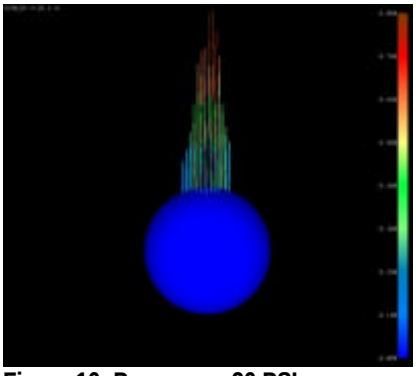

Figure 16: Pressure = 36 PSIg

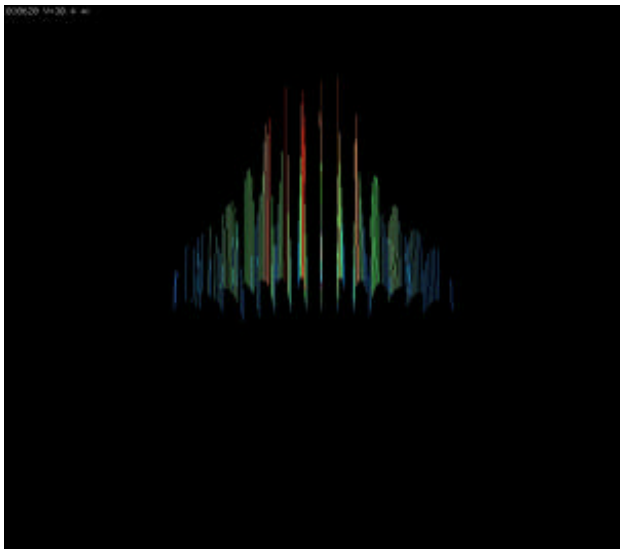

Figure 17: 3-D view of the displacement along the Y-axis for a pressure of 36 PSIg

6.3 Rupture and analysis of the displacements

The measurements are displayed as displacement vectors for each of the pressurization steps. In a second approach, the positions of the dots on the pattern are compared to the FEA results in an appropriate coordinate system. Finally, results obtained for positions of the dots are interpolated to the measurement of the displacement at the location of each strain gage; hence the strain and the displacement are correlated.

A tiny water leak appeared at a pressure of 31PSIg. Ultimately, the Absorber window completely failed at 44 PSIg. Figure 18 shows the window with the gash at the thin center, after having burst. A sound similar to tearing aluminum foil, followed by gurgle-gurgle gush-gush, as nearly eight liters of water spilled onto the optical bench, then onto the floor. Volunteers, some particularly qualified for this moment, seemed to disappear. After blotting the targets to remove the water (and mopping the floor), a final set of exposures was completed. After eliminating a few magnetic coded targets, which were floated by the cascading torrent, the agreement with the base set, as cited above, was quite acceptable.

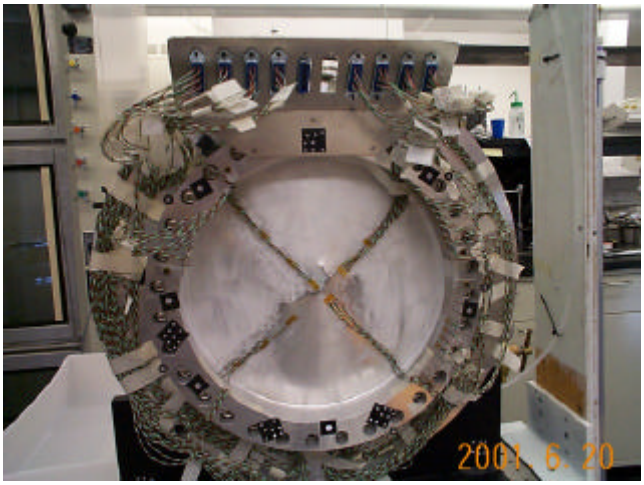

Figure 18: Rupture of the window

Figure 19 shows the correlation between the measured and calculated displacements. The calculation prediction agrees with the measurement results. The largest error is 10 % and the average of the error is 6.3 %, in the range 5 PSIg to 29 PSIg. The reproducibility of the measurement was investigated at two different stages of the test, with less than 5 μm of difference measured.

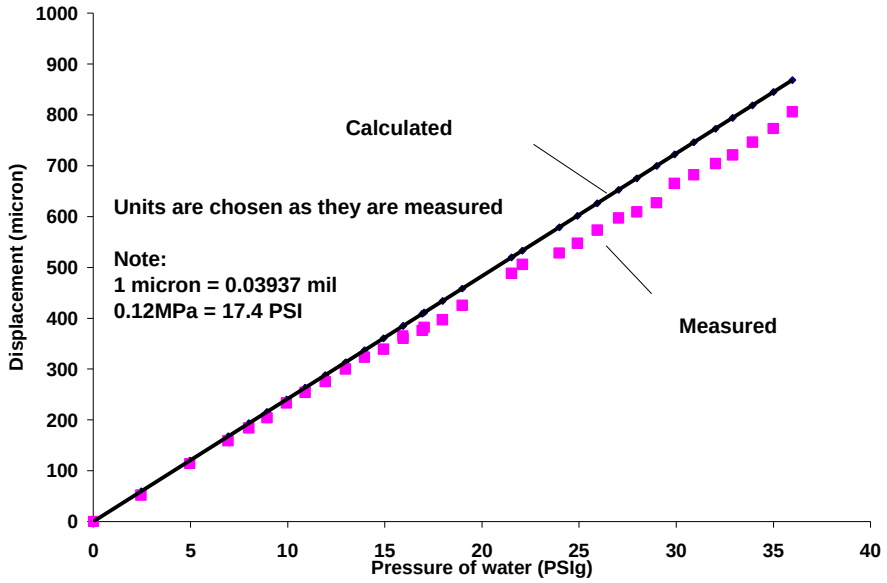

Figure 19: Correlation between the displacements measured and calculated Dot located at 17 mm from the center of the LH_2 absorber window

7 CONCLUSION

Success was declared at all levels:

- The displacements determined using photogrammetry are in close correlation with the FEA predictions.
- We destroyed the Absorber Window, as requested by the safety panel.
- The required precision (~0.010 mm) of the photogrammetry was achieved.
- The ability to acquire suitably accurate results in very short cycle-times was proven.
- After a few false starts, an acceptably stable setup was constructed that could be relied upon for several hours.

The photogrammetry technique has permitted us to obtain very accurate measurement of displacement during the pressurization test of a LH_2 Absorber window. These measurements validate the finite element analysis results and, therefore, the LH_2 Absorber window design. The measurements fit the calculations within 6.3 % of error in the elastic mode of the LH_2 Absorber window deformation. The reproducibility of the measurements is within a 5 μm error.
The test permitted us to gain knowledge in short cycle-time repetitive photogrammetric measurements. The non-contact measurement technique proved its reliability and can be foreseen as the main technique for the control of the LH_2 Absorber window production.

Acknowledgements

This work was supported in part by grants from the National Science Foundation, the Illinois Dept. of Commerce and Community Affairs, and the Illinois Board of Higher Education. This pressure test was performed at the Northern Illinois Center for Accelerator and Detector Development (NICADD) at Northern Illinois University in collaboration with the Illinois Institute of Technology, Northwestern University and University of Illinois, Urbana-Champaign. We would like to thank Sasha Dychkant, Mary-Anne Cummings (LH_2 Absorber Project manager physicist), Deborah Errede, Mike Haney, Donna Kubik, Stephanie Majewski, Laura Bandura, Lisa Rodriguez and Jay Hoffman and for their participation during the pressure test of the LH_2 absorber window. We acknowledge Steve Geer, Dan Kaplan, David Hedin and Heidi Schellman for their interest in the test procedure and the Mississippi University for the manufacture of the window.

References

[1] Ionization Cooling Research and Development Program for High Luminosity Muon Collider: Fermilab Conf 98/136

[2] Status of Muon Collider Research and Development and Future Plans: Fermilab-Pub-98-179

[3] http://tspc01.fnal.gov/darve/mu_cool/mu_cool_HP.htm

[4] Geodetic Services, Inc., V-STARS 4.2 User Manual, December, 2000

Appendix

The choice of absorber and window thickness is governed by a tradeoff between the energy loss and multiple Coulomb scattering in a material. The beam is "cooled" by energy loss; both transverse and longitudinal momentum is lost to collisions with atomic electrons but the longitudinal momentum is restored by the RF acceleration between the absorbers. Energy loss occurs when the muons in the beam electro magnetically interact with the electrons of the material and is governed by the Bethe-Bloch equation:

$$\frac{dE}{dx} = \frac{4N_o z^2 a^2}{mv^2}\frac{Z}{A}\left\{\ln\left[\frac{2mv^2}{I(1-b^2)}\right]-b^2\right\}$$

Where m is the electron mass, z is the charge (in units of the electron charge) and v the velocity of the particle, $\beta = v/c$, N_o is Avogadro's number, Z and A are the atomic number and mass of the material, and α is the electromagnetic fine-structure constant. The path length in the material, x, is measured in gm/cm^2. The quantity I is an effective ionization potential of magnitude $I = 10\ Z$ eV. The dependence of dE/dx on material is weak since Z/A is roughly 1/2 for all materials except hydrogen. Numerically dE/dx is 1–1.5 MeV cm^2 gm $^{-1}$ and one multiplies by the density to find dE/dx in units of MeV/cm. The relevant point for this discussion is that dE/dx depends on Z/A.

Unfortunately as the beam traverses the material multiple Coulomb scattering increases the beam's phase space. Multiple Coulomb scattering represents the scattering of the incident particle on the atomic nuclei. The root-mean-square angular deflection in a thickness of material x is given by the approximate formula

$$q_{RMS} = \frac{21MeV}{pc}\sqrt{\frac{X}{X_o}}$$

where X_o, the "radiation length," is given by

$$\frac{1}{X_o} = 4Z^2\frac{N_o}{A}a^3\left(\frac{(h/2p)c}{mc^2}\right)^2 \ln\left[\frac{183}{Z^{1/3}}\right]$$

and note the leading Z^2 dependence; hence as Z increases the scattering grows as Z^2.
We then see

$$\frac{\text{Degredation from Scattering}}{\text{Improvement from dE/dx}} \propto Z$$

and therefore the best choice is the lowest Z material, hydrogen.

We would therefore expect the correct choice for window material would be Beryllium. However Be is known to be highly toxic if inhaled, leading to Berylliosis, a disease of the lungs. Proximity of a fragile Be window to a liquid hydrogen target is therefore too dangerous to consider and Aluminum is therefore the material of choice.